destressing of the stope rock prior to mining. Destressing holes 100 mm in diameter and up to 30 m long were drilled into the orebody in a fan-shaped arrangement. These holes were blasted to fracture the orebody and relieve stress before actual stoping operations began. Mining through the preconditioned zone resulted in a greatly reduced release of seismic energy, and no rockbursting occurred (Blake, 1980a, 1980b and 1982). As mining progressed beyond the preconditioned zone, the release of seismic energy increased and rockbursting occurred.

Board and Fairhurst (1983) presented results that also confirm the advantages to be gained by large-scale preconditioning of a highly stressed sill pillar in their work at the Coeur d'Alene mine in Idaho. Both instrumentation and practical experience indicated that the pillar destressing initiated a non-violent failure of the sill pillar. The pillar was subsequently extracted successfully, with minimal seismic activity during pillar recovery. The details of how the destress resulted in a decrease in pillar stiffness were unknown. It was assumed that the creation of new fracture surfaces was not important but that the separation or dislodging of fracture surfaces from their original mating position was.

Makuch *et al.* (1987) reported on four destress blasts in rockburst-prone pillars at Campbell Red Lake Mine. Destressing reduced the potential energy by fracturing the pillar and allowing the hangingwall and footwall to converge. However, these experiments resulted in varying degrees of success.

O'Donnell (1992) reported on a destressing application in a development end at the 2195 m level of INCO's Creighton mine. It involved drilling and blasting 10 destress holes with each production round. Initially, problems associated with rockbursts occurring during working hours were experienced. The knowledge gained from these problems at early stages of the experimentation emphasised the importance of a proper sequence of development work and destressing. Subsequently, the judicious use of destressing, support, and mining sequence enabled three major blocks to be developed, with a significant reduction in the risk of rockbursts. Under adverse conditions, destressing induced 85 percent of the bursts to occur with the blasts.

Boler and Swanson (1993a & 1993b) explored the use of several measurement and analysis tools for evaluating the effectiveness of a sill pillar destressing attempt in Wallace, Idaho. The largest seismic event, which occurred just a few seconds after the destressing blast, was only a Richter magnitude (M) 0.4, despite the expectation of it triggering a significantly larger (M>1.5) event. An intensive instrumentation and monitoring programme was used, focusing on seismic and rock pressure changes. Numerical modelling was used to determine the stress interaction between the destressing blast and the two damaging events that occurred five days after the destressing blast. The rock pressure changes due to this ineffective destress blast were recorded as less than 100 kPa. However, several hundred kPa of pressure changes were measured during the following 18 days and most of this change was coincident with seismic events. The ability of close monitoring of the rockmass to determine the effectiveness of the destress blast was successfully shown and three main conclusions were drawn. These conclusions are set out below.

i. Adequate knowledge of the existing local stress field is necessary for designing appropriate hole patterns for destress blasts. Knowledge of the far-field stresses that may be affected by destressing may also be needed.
ii. Knowledge of the approximate principal stress directions allows the designing of the blasthole patterns for the most effective crack-growth pattern.
iii. Any means of monitoring the response of the rockmass to the destressing is highly desirable so that its effectiveness can be evaluated.

The technique of destressing for rockburst control has been utilised with apparent success at Campbell Red Lake Mines Ltd. However, it is recognised that the need exists to improve the understanding of rockmass response to blasting, upon which destress blast design is based (Scoble *et al.*, 1987).

Coal Mines

Coal mines, particularly in Poland and Germany, are prone to gas outbursts and translatory rockbursts (Burgert & Lippmann, 1981). Gas outbursts are probably more common in coal mining but there are occurrences in other mines, too. The

common destressing practice in Polish coal mines is to drill long boreholes into the seam to allow the gas to dissipate (Kozlowski and Sierkiewicz, 1977 and 1981; Krawiec, *et al.*, 1977; Tarnowski, 1978; Fenc, 1979a, 1979b, 1980, 1981). Under certain circumstances, water is forced into the coal and controlled blasting in the boreholes is also carried out. Both of these techniques decrease the coal strength, thus destressing or preconditioning the coal seam. In addition, the blasting creates fractures, which permit gas to escape (Bräuner, *et al.*, 1976; Baule, 1977; Rudnicki, *et al.*, 1977; Ward, 1980).

The rockbursts in the Ruhr coalfield, Germany, are associated with a sudden movement of the seam into the underground openings because of high-stress concentrations nearby. Bräuner (1974) reported a successful destressing experiment in a roadway which was driven in a particularly burst-prone part of a seam. Significant stress reductions were achieved by drilling destressing holes in areas where stress concentrations were reaching dangerous levels. The boreholes were not blasted but the destressing was attained by releasing large quantities of broken coal. The 95 mm-diameter destressing holes yielded up to 14 m^3 broken coal per metre drilled whereas the normal quantity to be expected from this size of hole in unstressed coal is only 10 lt per metre drilled. Finally, 540 m^3 coal were thus removed over a road length of 80 m, and the roadway remained stable.

Lama (1972) showed a case example on the use of a destressing technique in the maintenance of roadways under high stresses. A number of 32-35 mm-diameter and 2.5-3.0 m-long destressing holes were drilled and blasted into the sides and floor of a roadway lying at a depth of 1200 m driven in carboniferous shale beds. The movement of the floor and side walls greatly decreased, with a significant reduction of load on the roadway support.

Seismic monitoring is used in German coal mines in order to identify conditions under which preconditioning of the coal seam can be beneficially carried out (Will, 1982). The preconditioning is done by drilling 100 mm diameter holes 25 m long, parallel to the coal face. The holes are drilled from a roadway and are 2 m apart, starting 3 m ahead of the face. High stresses in the coal appear to be relieved by the coal fracturing into the holes.

Piguet (1982) and Will (1982) described how destressing of a coal seam was carried out after a rockburst had been predicted by precursive criteria using a seismic monitoring system (Dechelette, *et al.*, 1982). Shadrin (1984) showed a close correlation between microseismic activity and the rate and pressure of fluid pumped into a coal seam for the purposes of destressing and preventing gas emission. He concluded that the microseismic activity was the result of the formation of new fractures by the pressurising fluid.

Haramy *et al.* (1988) discussed some of the destressing techniques used in U.S. coal mines. They described destress blasting as "volley firing". The destressing holes were drilled into previously located high-stress zones at the longwall face but no detail was given on the determination of those highly stressed areas. The numerical modelling analysis showed that destressing only a portion of the face redistributed the stresses to adjacent areas that were not destressed, and resulted in dangerous high-stress conditions at those locations. Another destressing technique used in U.S. coal mines was "auger drilling". In this method, stress relief was induced by drilling large-diameter holes into a highly stressed area. A hole or series of holes in a coal seam would structurally weaken the seam and cause failure of the coal at a reduced stress level; stress build-up cannot then occur.

In China, Jianyun and Jiayou (1988) reported a number of rockburst occurrences at various underground workings such as coal mines, metal mines, hydropower stations and railway tunnels. They described the methods commonly used for rockburst prediction and control and explained the efforts made to eliminate the rockburst occurrence through the use of better mining methods and layouts, as well as through destressing techniques such as preconditioning blasts, high-pressure water injection and drilling of destressing holes. Preconditioning techniques were used successfully in four coal mines (Mentougou, Longfeng, Tangshan and Tianchi mines) and, to a limited extent, at some metal mines.

2.6 Summary

An earlier and less comprehensive version of this literature review was conducted to record major outcomes of rockburst control attempts in different mining environments in the world. Collecting this information was a crucial step for CSIR / Miningtek's rockburst control research project as it became a baseline and a major tool for determining the direction for further research in this area. This review was also a very important step for determining an initial preconditioning layout at CSIR / Miningtek's site investigations.

The literature review revealed that there were a very limited number of documented cases (e.g. Roux *et al.*, 1957 and Hill and Plewman, 1957) that were directly related to the South African deep-level mining environment. Although very positive and encouraging results were documented by the above-mentioned authors, they were not sufficient for convincing the South African gold mining industry to implement this technique on a wider scale. This was probably because of the limited quantification of the effects of the destressing (preconditioning) technique at ERPM. While the South African gold mining industry was not interested in implementing this potentially very effective technique, many other countries (e.g. USA, Canada, Poland, Germany, etc.) were testing a variety of destressing techniques in different mining environments with varying degrees of success.

As was explained in Section 1, rockbursting has been a continual hazard for South African deep-level gold mines and the accident rates due to rockbursts were unacceptably high. Therefore, a CSIR / Miningtek research team was assigned to develop rockburst control techniques to minimise the damaging effects of these and to create a safer working environment for mining personnel. This Ph.D. thesis forms only a part of this broadly defined research programme and shares its objectives.

3 THE EFFECTS OF PRECONDITIONING BLASTS IN CONFINED ROCK

3.1 Introduction

The main objective of the rockburst research programme of the Chamber of Mines Research Organisation (COMRO, now CSIR / Miningtek) was to develop rockburst control methods, to enable mines to operate safely in areas which are most at risk from seismicity and the resulting rockbursts. Research work on preconditioning as a rockburst control technique was carried out in various deep-level gold mine stopes. Initially, the preconditioning blast designs were based on a limited understanding of the actual effect of the explosives on the rock in the confined and highly stressed conditions ahead of the stope face. Evaluation of the preconditioning method relied on the observation of the effects that were produced by a preconditioning blast. The cost of drilling and blasting for preconditioning was high and successes have been accomplished by using high powder factors and blasthole layouts determined by trial and error. To minimise the cost and enhance the success of preconditioning, there was an obvious need for designing and planning the blasts. Preconditioning blast design had to be based on knowledge of the actual effect of the explosives on the rockmass in the confined and highly stressed conditions and on an understanding of the mechanisms of preconditioning.

Although the preconditioning techniques were primarily considered for stopes, the experiment described in this section examines the effect of the explosives in a confined and highly stressed rockmass ahead of a tunnel. In order to better control the test blasts and not to disrupt the production in a stope, a remote tunnel was chosen as an experimental site, instead of a stope. In this tunnel a number of dynamic and static measurements were made, close to different explosive charges in confined and highly stressed rock. The information obtained from these blasting experiments helped in the understanding of the interactions between explosive and rock and was very useful later in designing effective

preconditioning blasts in stopes and for use in the modelling of preconditioning blasts using computer codes.

3.2 Objectives

The design of preconditioning blasts (charge mass, charge type, hole spacing and diameter, position of charge in the rock and the initiation of charges) required a good knowledge of the effect of explosives on rock. Dynamic computer codes could provide insights into the effect of explosives on rock under confined conditions but no physical measurements had been made of the effects of explosives under such conditions.

The objective of this work was to determine the influence of blasting in confined rock ahead of a tunnel face so as to obtain information on which the design of preconditioning blasts in highly fractured and stressed rock ahead of a stope face will be based. Therefore, this work was essential in providing the basic understanding that was required for designing effective preconditioning blasts.

In order to achieve this objective, four preconditioning test blasts were detonated and monitored. The blast parameters were varied and these were: explosive type, explosive quantity, hole length, hole diameter, stemming, and charge length.

3.3 Test programme

In order to keep the measurements as simple as possible and the number of variables to a minimum, only one borehole was drilled, instrumented and blasted per test.

The South African Gold Mining Industry uses mainly two common types of explosives: ANFO (Ammonium Nitrate Fuel Oil mixes), and emulsion explosives. Initially, it was planned to test three or more types of explosives. However, in order to minimise the number of tests, it was decided that only those two

common types of explosives would be tested rather than the full range available on the market.

The energy partitioning is affected by the charge diameter and by the mass of explosives in the holes. Therefore, different blasthole diameters produce varying effects on the surrounding rock. In order to evaluate these effects, the explosives were charged and detonated in two different hole sizes (e.g. a small diameter hole of about 61 mm and larger diameter holes of about 93 mm).

Blasting results in terms of fracturing mechanism and the extent of fracturing are also dependent upon the charge position ahead of the face and the level of confinement. Previous studies at actual in-stope preconditioning experiments have shown that the effectiveness of the preconditioning blasts vary for different charge positions ahead of the face. In order to study these effects in a better controlled test site, two different hole lengths (e.g. short holes of about 4.7 m and a longer hole of 5.5 m) were tested.

For better control on blasthole parameters such as blasthole diameter, length and direction, it was necessary to diamond drill all the holes. For the installation of accelerometers and strain gauges, the bottoms of the monitoring holes were flattened, following which a smaller diameter, short hole (stub) was drilled to house the transducers. This allowed for overcoring and instrument retrieval.

The production blasts were controlled so that a minimum of additional fracturing was introduced. To ensure that accurate measurements were taken, the face advance through the pre-blasted rock was a maximum of 1 m per production blast. This allowed detailed fracture mapping of the face after each production blast and the retrieval of monitoring transducers for possible re-use in the subsequent tests.

3.3.1 Test site

For ease of access and speed of completing the programme, it was decided that this work would be carried out in a remote development end on 38 level of 6

Shaft at West Driefontein Gold Mine where stress levels were expected to be relatively high. For reliable comparisons between tests, it was necessary for the face to remain in similar rock and stress conditions throughout the experiment. In order to achieve this, the site was established in a breakaway from the main haulage with sufficient development to bring the tunnel to the position from which further development could be carried out along a straight line parallel to the strike.

3.3.2 Instrumentation and monitoring

The most important issues to be examined in terms of understanding the effect of explosives on the rockmass are the detonation speed of the explosive and resultant gas penetration characteristics, the total energy imparted to the rock which is related to the explosive type and charge mass, and the level of confinement.

The effects of an individual blast were observed through the steps that are set out below.

- Monitoring the blast by acceleration measurements at various distances from the blasthole was carried out to provide information on shock energy entering the rock. Six accelerometers were installed for each blast at different distances around the blasthole.
- Strain measurements in the rock were taken at three radial distances from the blasthole before and after the blast. Doorstoppers, which are strain gauges installed in an acoustically coupled medium, were used for these measurements.
- Strain measurements were taken to determine the static stress field for use in modelling and to capture any major changes in stress field throughout the investigations.
- The Velocity of Detonation (VOD) of the explosive was measured by using a VOD meter.
- Stereo-photography of the face was taken for the purpose of mapping the blast-induced fracturing after each advance of the tunnel face.

- Studies on rock core samples (e.g. Rock Quality Designation (RQD), and strength characteristics of the rock) were carried out before and after a preconditioning blast.
- Ground Penetrating Radar (GPR) surveys were used to examine the effect of the blasts on fracturing.

3.4 Blast monitoring

3.4.1 Introduction

Four preconditioning test blasts were carried out in the test site. In all these test blasts, a single borehole was charged, detonated and monitored. The details of the parameters used for these preconditioning test blasts are summarised in Table 3.4.1.

Table 3.4.1 Detail of blast parameters

DESCRIPTION	BLAST 1	BLAST 2	BLAST 3	BLAST 4
Explosive Type	Anfex - ANFO (Blow-loaded)	Emex ED7 (Cartridges)	Prillex - ANFO (Blow-loaded)	Prillex - ANFO (Blow-loaded)
Hole Diameter (mm)	61	93	93	93
Hole Depth (m)	4.75	4.70	4.66	6.50
Charge Length (m)	1.95	1.76	1.60	2.52
Charge Mass (kg)	6	12	12	12
Density (kg/m^3)	1050	1004	1100	700
Total Energy Output (MJ)	17	42	34	34
Stemming Length (m)	2.80	1.80	3.05	2.98
Stemming Material	Clay (Tamped)	Clay (Tamped with cone)	Bentonite mixture (Tamped)	Bentonite mixture (Tamped)
Initiation System	Nonel with detonator at toe of hole			

Note: The density of blow-loaded ANFO is dependent on the softness of the drill and the air pressure at the time of charging.

In the second test blast, a special aluminium cone device was placed in the stemming to try to increase the stemming retention time. The purpose of

maximising the retention time is to contain the energy of the explosives in the hole as long as possible.

Figure 3.4.1 is an amalgamation of four test blasts and illustrates the blastholes in section. Using a hole diameter of 93 mm, and a charge length of 1.78 m for the second blast, the effective in-hole density of the emulsion ED7 was only 1004 kg/m^3 even though the cartridges were well tamped with a charging rod. The blow loading of the ANFO in the third blast (12 kg at a density of 1100 kg/m^3) resulted in a shorter column length than the 12 kg of ED7 cartridged emulsion, which had an in-cartridge density of 1290 kg/m^3. This indicates better coupling of the ANFO in the third test blast. However, the same amount of ANFO, in the fourth test blast, resulted in a longer charge column and thus a lower explosive density. This was because of low air pressure and / or poor charging practice when using the ANFO loader. The effects and results of the low explosive density in the fourth test blast will be discussed in later sections.

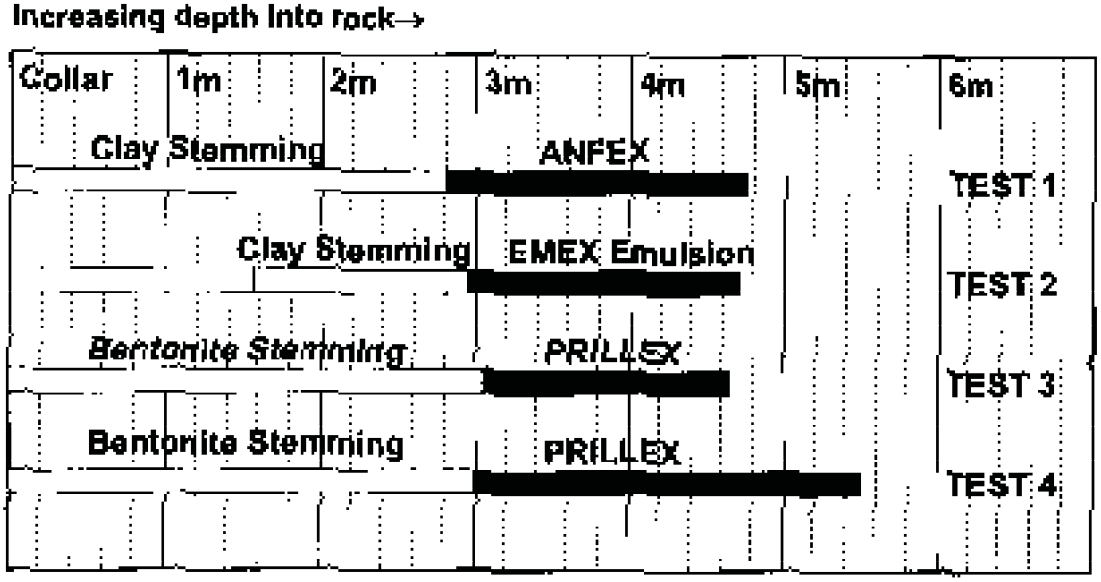

Figure 3.4.1 Scaled section of the blastholes from each test

3.4.2 Instrumentation

For the first preconditioning test blast, six accelerometers were grouted into holes around the charge. Each accelerometer was inserted into a purpose-made

aluminium boat which was buried in a tungsten cement (a mixture of tungsten powder and cement) at the end of each instrument hole. Figure 3.4.2 shows the instrument hole locations relative to the blasthole.

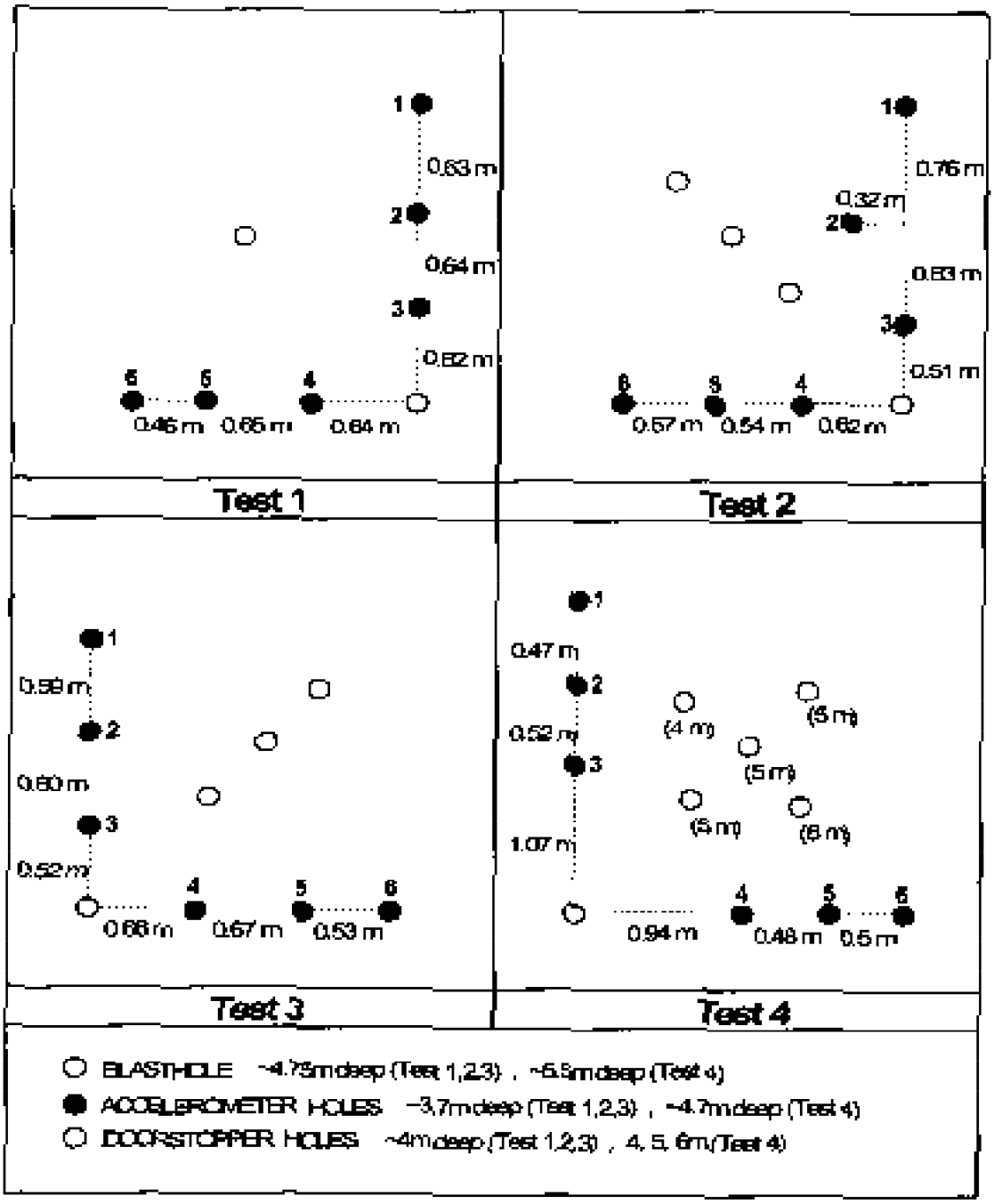

Figure 3.4.2 Schematics of the tunnel faces, showing the relative positions of the blasthole, accelerometer and doorstopper holes

A 150 mm-long stub hole with a diameter of 48.3 mm was drilled at the end of each hole to house the accelerometer (Figure 3.4.3) to allow over-coring and

recovery of the instruments. The boats were installed and aligned by means of 50 mm-diameter PVC drain pipes. Each accelerometer was oriented so that the base pointed towards the blasthole and was located approximately opposite the centre of the charge length.

The accelerometers used were PCB Series 305A units which can measure up to 1.0×10^6 m/s^2. They were connected to a Blast Analyser, an eight-channel, portable, high-speed digital recorder. The sampling rate was set at 250 kHz on each channel.

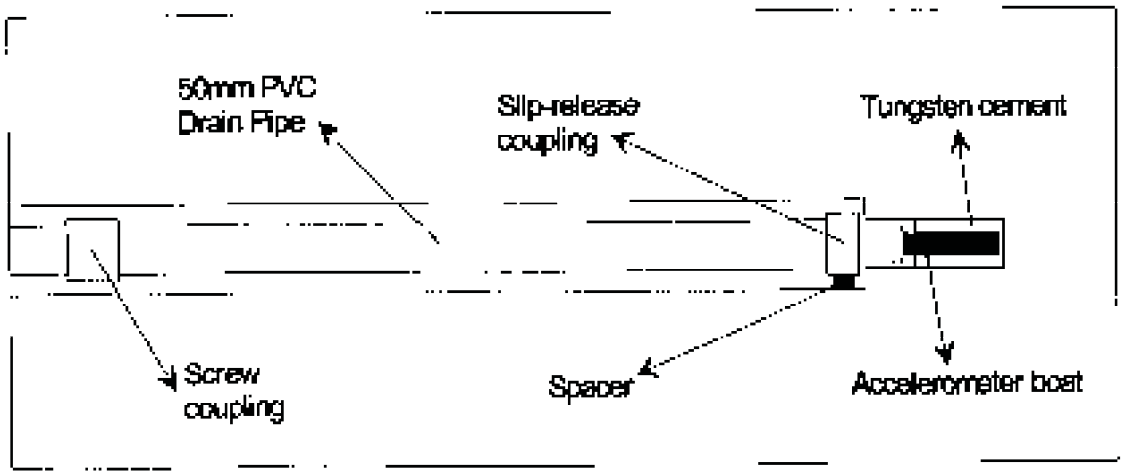

Figure 3.4.3 Schematic section through an instrument hole, showing the installation technique for accelerometers

Velocity of Detonation (VOD) measurements were carried out at seven intervals in the blasthole by using a VODEX instrument which measures VOD at a measurement accuracy of 1.0×10^{-6} second using 16-way ribbon cable. The first measurement point was attached to the detonator and the intervals between subsequent measurement points were 170 mm. The last sensor point was located at the collar of the hole to determine the effectiveness of the stemming. The purpose of taking VOD readings was to enable comparisons with future tests in terms of detonation velocity and stemming retention time. These are factors that control the explosive energy imparted to the rock and the containment period of the energy in the hole.

For the second test blast, similar instrumentation was used as in the first test blast, except that the portable high-speed digital recorder was set at a sampling rate of 500 kHz per channel and the intervals between the VOD measurement points in the explosives column were 300 mm. In this test blast, two additional horizontal geophones, sensor SM6 units, were cemented to the tunnel sidewalls at a distance of 50 m from the blasthole. They were connected to the two remaining channels of the high-speed recorder. The sampling rate for these two instruments was set at 5 kHz with a recording period of 30 seconds. The purpose of these geophones was to determine if there were any related or triggered seismic events shortly after the blast.

Instrumentation for the third and fourth test blast was similar to that for the second test blast, except that the drill hole pattern for the blasthole and the instrumentation holes were mirror images of those for the second test blast (Figure 3.4.2). The reason for this was to ensure that the blasthole in the third test blast was outside the zone of influence of the second test blast in which the tunnel was highly damaged.

In the fourth test blast, the blasthole parameters were kept the same as for the third test blast, with the exception that the depths of holes were almost 1 m greater.

3.4.3 Results of blast monitoring

In the first test blast, spalling of the face occurred in the vicinity of the blasthole. This spalling was due to the reflection of the blast-induced shock waves off the face.

The total energy released by the explosives in the second test blast was more than double the energy released in the first blast. This was evident in significantly higher acceleration readings and severe damage to the instrument holes closest to the blasthole. Two of these holes (i.e. closest to the blasthole) were completely closed after the blast. The damage may have been related to gas-energy penetration as well as shock-energy reflection from the blasthole sidewalls.

Damage at the tunnel face was also more intense than in the first blast, with about 20 cm to 30 cm thickness of rock spalling off the entire tunnel face.

In the third and fourth blasts, the face damage was not as severe as that in the second blast and there was only limited face spalling. After the third test blast, it was observed that the instrument holes closest to the blasthole were damaged in the portion opposite the charge. The fourth test blast was planned to be a repetition of the third test blast, except the depths of holes were almost 1 m greater. Despite the fact that the calculated total energy to be released by the explosives in the fourth test blast was the same as that calculated for the third test blast, the lower explosive density in the charge column resulted in much lower detonation pressure in the fourth test blast. As a result of this, the damage on the face was negligible.

Seismic measurements

No seismic events were detected within 30 seconds of the detonation. The peak values obtained from the detailed acceleration data and the computed peak velocities and strains are tabulated in Table 3.4.2.

The peak velocity values were obtained by integrating the acceleration data, and the peak strains were computed from the obtained peak velocities using equation (1).

$$\varepsilon_p = V_p / C_p \quad \text{.....(1)}$$

where ε_p = peak strain

V_p = peak velocity

C_p = P-wave velocity (5500 m/s)

The following information can be inferred from the data.

- There is a progressive decrease in peak accelerations (i.e. shock energy) and peak velocities away from the blasthole (Figure 3.4.4 and Figure 3.4.5).

- The peak values for acceleration and velocity are higher for the vertical array. This is probably a function of the higher vertical component of the field stress (Figure 3.4.4 and Figure 3.4.5).

Table 3.4.2 The peak accelerations obtained from the test blasts

TEST BLAST	CHANNEL NUMBER	PEAK ACCELERATION (m/s^2)	PEAK VELOCITY (m/s)	PEAK STRAIN (10^{-6})
Blast 1 (6 kg Anfex)	1 (Vertical)	39160	1.9	345
	2 (Vertical)	49438	4.3	782
	3 (Vertical)	98295	6.6	1200
	4 (Horizontal)	82960	9.1	1655
	5 (Horizontal)	30468	2.5	455
	6 (Horizontal)	25349	1.3	236
Blast 2 12 kg Emulsion)	1 (Vertical)	145178	3.4	618
	2 (Vertical)	344371	7.5	1364
	3 (Vertical)	843620	17.9	3254
	4 (Horizontal)	510416	11.5	2091
	5 (Horizontal)	No reading	-	-
	6 (Horizontal)	162037	3.5	636
Blast 3 (12 kg Prillex)	1 (Vertical)	426633	6.0	1091
	2 (Vertical)	454412	10.6	1927
	3 (Vertical)	576309	11.7	2127
	4 (Horizontal)	No reading	-	-
	5 (Horizontal)	No reading	-	-
	6 (Horizontal)	175957	2.6	473
Blast 4 (12 kg Prillex)	1 (Vertical)	35257	0.009	0.55
	2 (Vertical)	44066	0.283	51.45
	3 (Vertical)	79283	0.543	98.73
	4 (Horizontal)	96981	1.089	198
	5 (Horizontal)	No reading	-	-
	6 (Horizontal)	44060	0.149	27.09

- The peak accelerations in the third test blast are higher than those in the first test blast (Figure 3.4.4).
- Compared to the second test blast, the peak accelerations in the third blast are lower closest to the blasthole, but significantly higher further from the blasthole (channel 1 & 2). The rate of attenuation in peak acceleration in the third blast is therefore much lower than that in the second blast (Figure 3.4.4).

  The lower rate of attenuation in peak acceleration implies that a much larger volume of rock should have been influenced by the blast. The reason for the lower rate of attenuation is not clear, but can probably be related to the lower velocity of detonation and the 100 percent coupling provided by the blow loading of the ANFO in the third test blast.
- Although 12 kg of ANFO was detonated in the fourth test blast, the low explosive density in the charge column resulted in the peak acceleration values being as low as in the 6 kg ANFO blast (1st test).

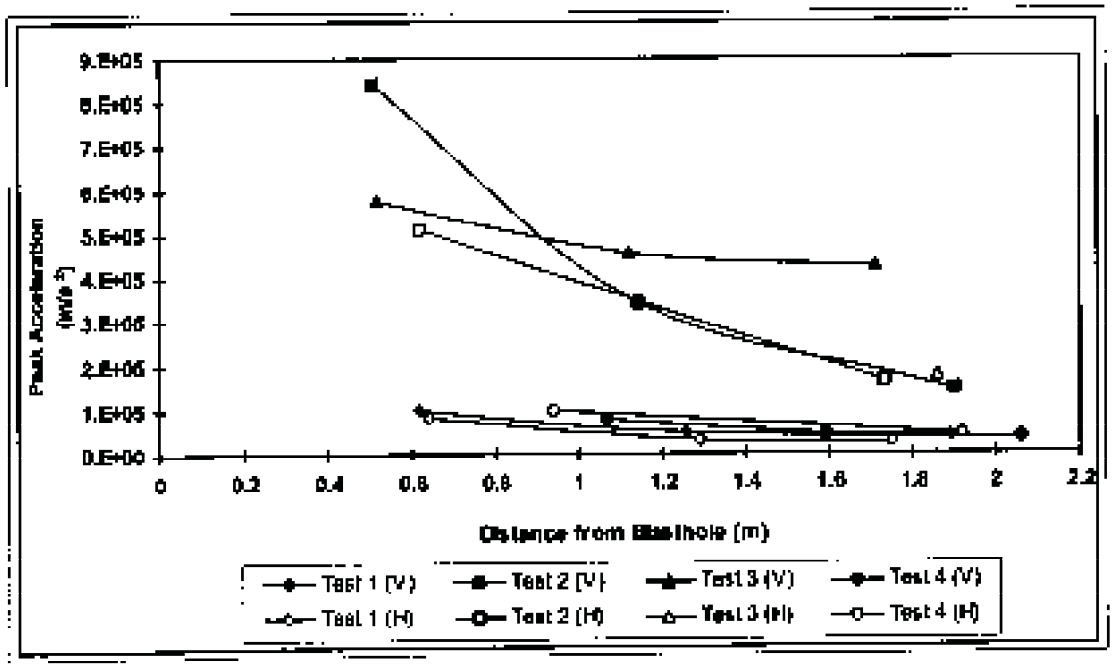

Figure 3.4.4 Peak accelerations vs. distance from blasthole

Velocity of Detonation (VOD) measurements

The detonation velocities measured during the first test blast are given in Table 3.4.3. Spacing between sensor positions in the blasthole was 170 mm. The data

shows that detonation was relatively constant, with an average value of 3757 m/s. A sensor point was located at the collar of the blasthole to give the time duration before the stemming was ejected from the hole collar. The stemming retention period was 2.8 x 10^{-3} seconds, which corresponds to 1.43 x 10^{-3} seconds/metre of retention rate.

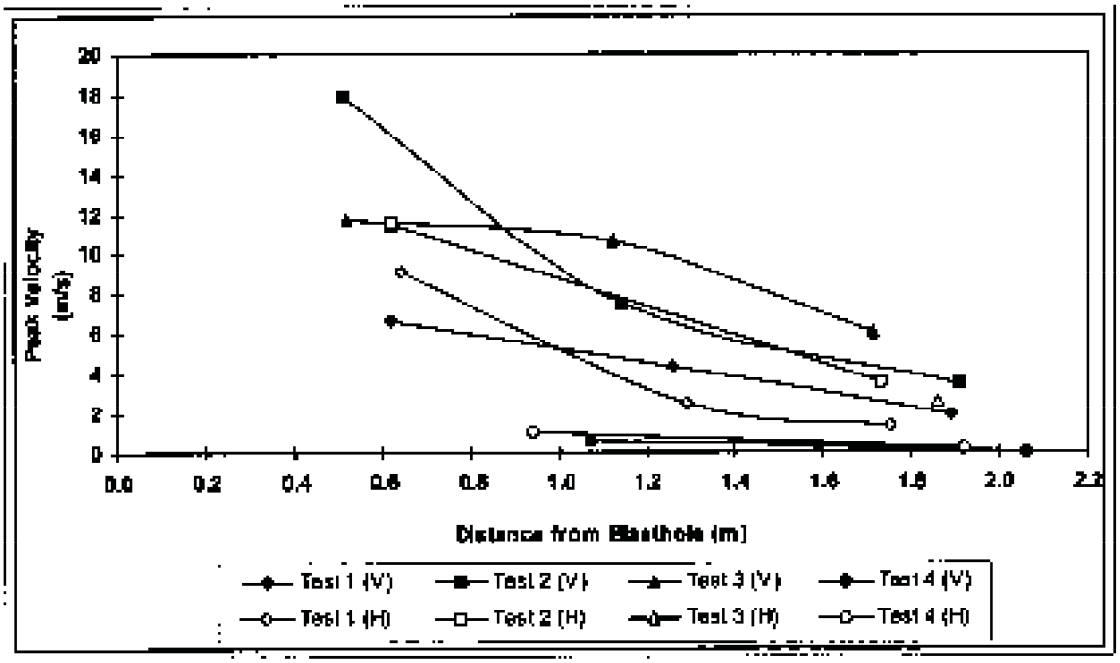

Figure 3.4.5 Peak velocities vs. distance from blasthole

The detonation velocities measured during the second test blast are given in Table 3.4.4. Unlike the first test blast, the spacing between the VOD sensor points in the blasthole was 300 mm. A relatively low reading at sensor point 7 was because this sensor was located in the stemming material and it was not included in the calculation of average VOD. The remaining data indicates that detonation velocity was relatively constant throughout the explosive column, with a mean value of 5719 m/s. This is significantly higher than the mean VOD of 3750 m/s obtained for ANFO in the first test blast. The higher VOD indicates that the explosive used in the second test blast imparted a larger proportion of shock energy to the rock than did the first test blast. Shock energy is defined as the energy following detonation to the point where radial expansion of the blasthole results in the explosive pressure being matched by the field stress in the rock. Shock energy produces micro fractures and crushing of the rock around the

blasthole. Gas energy follows the shock energy in time and penetrates the fractures, thus extending them into long visible cracks.

Table 3.4.3 The detonation velocities measured during the first test blast

CHANNEL NUMBER	CUMULATIVE DISTANCE (mm)	VOD (m/s)	TIME (10^{-3} seconds)
1-2	85	3400	50.0
2-3	255	3711	45.8
3-4	425	3872	43.9
4-5	595	3990	42.6
5-6	765	3911	44.8
6-7	935	3761	45.2
Mean VOD		3757	
Stemming retention rate		1.43 x 10^{-3} s/m	

Table 3.4.4 The detonation velocities measured during the second test blast

CHANNEL NUMBER	CUMULATIVE DISTANCE (mm)	VOD (m/s)	TIME (10^{-3} seconds)
1-2	300	5940	50.5
2-3	600	5671	52.9
3-4	900	5504	54.5
4-5	1200	5736	52.3
5-6	1500	5747	52.2
6-7	1800	* 3554	84.4
Mean VOD		5719	
Stemming retention rate		1.04 x 10^{-3} s/m	

The measured stemming retention rate of 1.04 x 10^{-3} s/m during the second test blast was lower than that recorded in the first test blast (1.43 x 10^{-3} s/m) in spite of the conical device placed in the stemming. The reduced retention rate was

probably a function of the increased hole diameter, and the shorter overall length of hole stemmed.

The detonation velocities measured during the third test blast are given in Table 3.4.5. The readings were relatively constant throughout the explosive column with a mean value of 4400 m/s. This is higher than the mean VOD of the first ANFO blast (3750 m/s) and lower than the mean VOD of the emulsion blast (5700 m/s). The lower VOD levels indicate that peak shock energy levels should have been sustained for longer. This is confirmed by the readings obtained from the accelerometers, as shown in Table 3.4.2 and Figure 3.4.4.

Table 3.4.5 The detonation velocities measured during the third test blast

CHANNEL NUMBER	CUMULATIVE DISTANCE (mm)	VOD (m/s)	TIME (10^{-3} seconds)
1-2	300	4120	72.8
2-3	600	4437	67.6
3-4	900	4316	69.5
4-5	1200	4566	65.7
5-6	1500	4518	66.4
6-7	1800	-	-
Mean VOD		4391	
Stemming retention rate		3.08×10^{-3} s/m	

The stemming retention rate was measured at 3.08×10^{-3} s/m. This was significantly higher than that obtained from the first and the second test blasts, at 1.43×10^{-3} s/m and 1.04×10^{-3} s/m respectively. Long retention times are better for containing explosive energy in the rock for as long as possible, resulting in better extension of cracks in the rock. The bentonite stemming material was mainly responsible for improved retention time. Slightly longer stemming length might have also contributed to the improved retention time.

The measured detonation velocities from all test blasts, except the fourth test blast, are illustrated graphically in Figure 3.4.6. In the fourth test blast, no VOD

measurement was obtained, because the Nonel detonators in the stemming inadvertently cut the Vodex sensor cable before the charge fired.

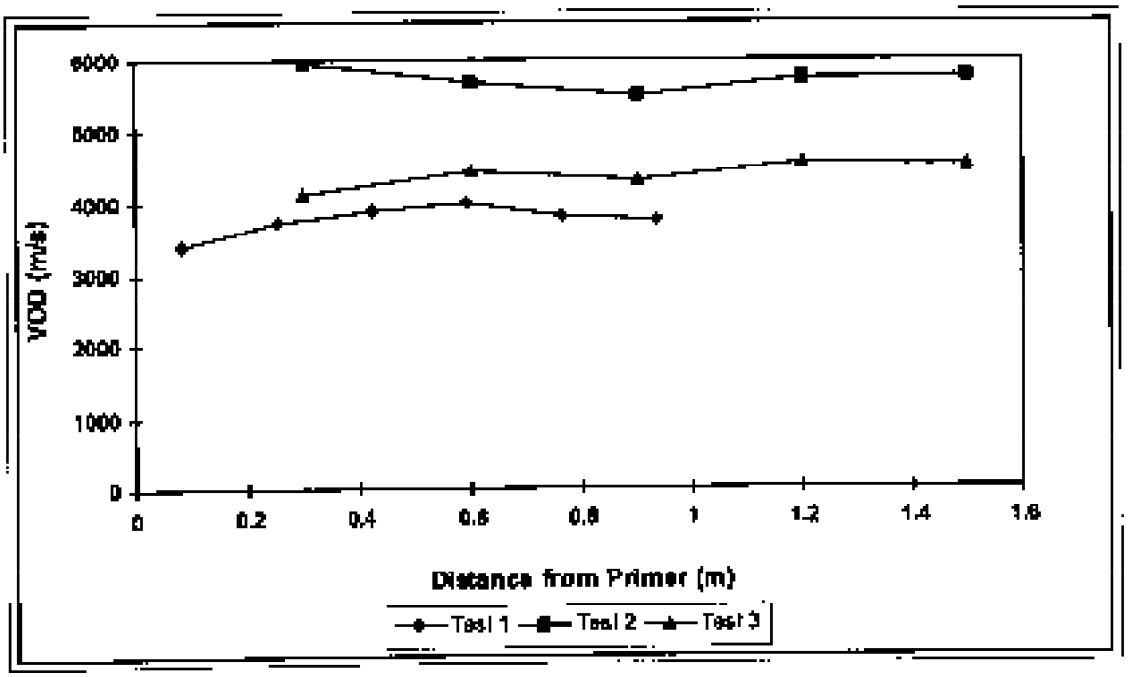

Figure 3.4.6 The detonation velocities measured during the 1st, 2nd and 3rd test blasts

3.5 Ground Penetrating Radar (GPR) Investigations

The objective of the Ground Penetration Radar (GPR) investigations was to provide fracture profiles ahead of the development end before and after preconditioning blasts. A comparison between these profiles should allow semi-quantitative assessment of the effect of preconditioning blasts on rock fracturing.

A total of four GPR surveys were conducted for the third preconditioning blast in the period from July to October 1992. Although the survey results were satisfactory before the blast, data obtained after the blast was strongly influenced by the presence of doorstoppers and accelerometers in the rockmass. It was found, in particular, that the wiring connecting instruments interfered with the GPR so that comparisons between data obtained before and after the blast were limited.

Three GPR survey lines were selected along the rock face of the development end. Profile lines were located approximately 0.7 m, 1.4 m and 1.9 m above the footwall, and each profile line was scanned twice using different probing depth settings. The shallow setting refers to a depth of approximately 5.5 m, while the deeper setting approximates a depth of 7.5 m. Figure 3.6.1 shows the GPR scans with a shallow setting (5.5 m deep) taken before and after the third test blast.

It was observed that fracture density increased and that some fractures which were mapped on the pre-blast profile were more pronounced after the preconditioning blast. This implies that these fractures were widened and remobilised by the blast. It was also observed that new interfaces had formed while others appeared to be less pronounced or had even disappeared on the post-blast GPR profiles.

Intensification of fracturing in the top profile, which is further away from preconditioning blasthole, was also observed, but this appears to be less pronounced than in the other two profiles.

3.6 Production blasts and fracture mapping

Immediately following the first preconditioning test blast, fluorescent dye was pumped into the preconditioning hole in order to permeate the fractures that may have been formed by the blast. The attempt was to make those fractures formed by the preconditioning blast distinguishable from those formed by the production blast.

As was indicated earlier, the production blasts were designed to minimise the creation of additional fractures while advancing the tunnel. The first production blast was initiated with 100 holes, each 1 m long, which removed the rock cleanly from the face. After the first production blast the effectiveness of the round was assessed and the spacing between holes was increased. The second production blast had a total of 64 holes on an 8x8 square pattern. This blast was successful as it did not induce additional blast fractures in the rock. The two 100 mm holes

that were located diagonally opposite the corner of the preconditioning hole were used as free breaking points for the blast.

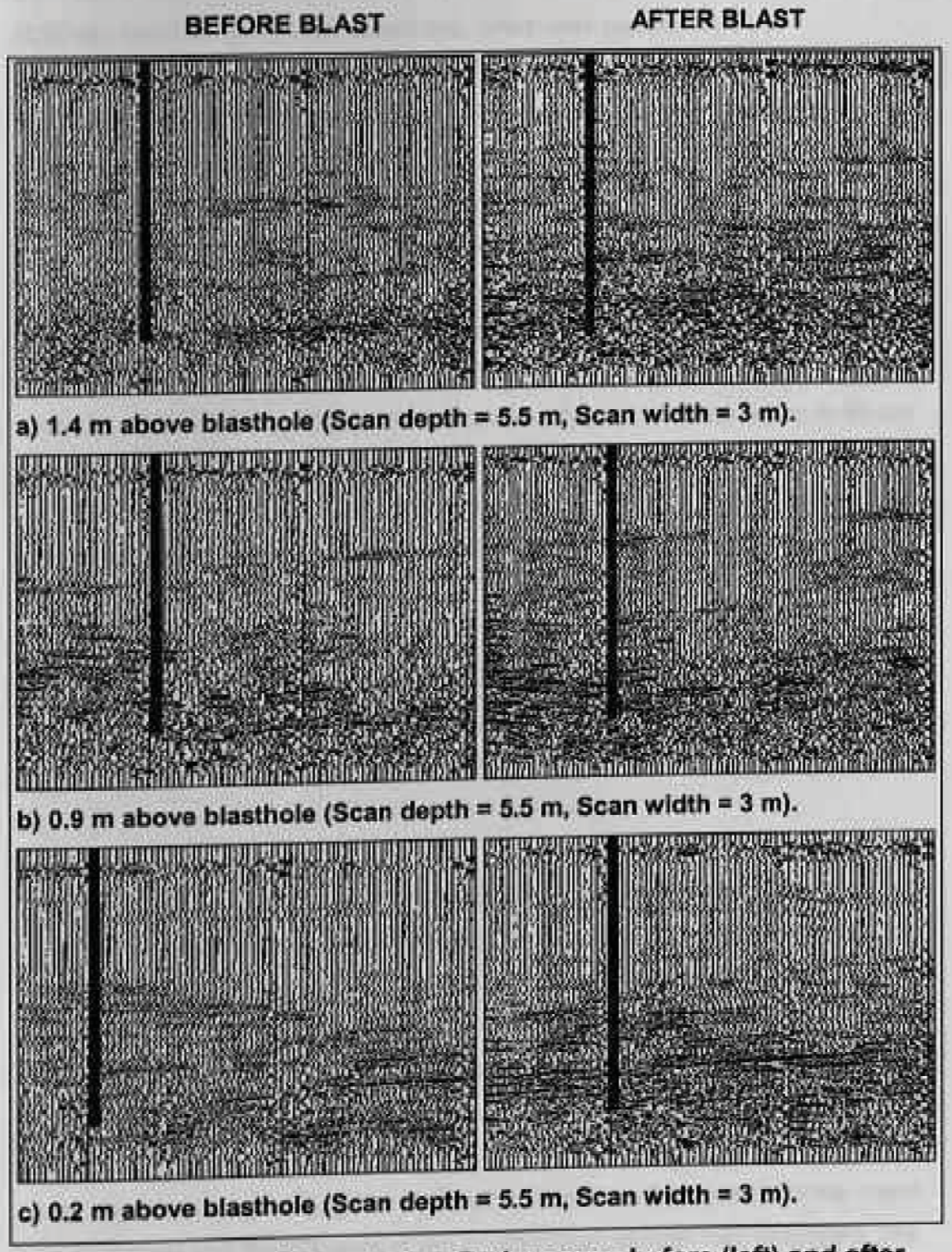

Figure 3.6.1 Ground Penetrating Radar scans before (left) and after (right) the third test blast

Note: Blasthole is shown by a black line.

After the second production blast the radial fractures initiated from the preconditioning blasthole were clearly visible on the tunnel face. In order to make sure that those fractures were created by the preconditioning blast, an ultra-violet light was used to locate fluorescent dye, which was pumped into the preconditioning blasthole immediately after the first test blast. A few visible radial fractures which extended up to 60 cm from the blasthole were observed. It was clear that the dye did not penetrate up to the tips of the fractures as they were traced up to 60 cm from the blasthole. Stereo-photographs of the preconditioning hole, the face and both sidewalls were taken for fracture-mapping purposes.

The third and fourth production blast rounds were designed in the same way as the second one. After the third production blast, it was observed that few visible radial fractures extended up to 100 cm and the dye spots extended up to 60 cm from the preconditioning hole (Figure 3.6.2). The fourth blast round was the last production blast for the first preconditioning blast. This blast exposed a small-scale fault. There was no indication of fracturing by the preconditioning blast on the fault surface.

After the production blasts following the first preconditioning blast were completed, the tunnel was developed about 4 m to get away from the zone of influence of the first test blast and to prepare the face for the second test blast. In fact, this process was repeated after each test blast.

Unlike the first test blast, two different colours of dye were pumped into the preconditioning blasthole, just before and immediately following the second, third and fourth test blasts, in order to permeate the pre-existing fractures and the fractures that may have been formed by the test blast. The intention was that the fractures formed by the preconditioning blast should be distinguishable from both pre-existing fractures and those formed by the production blast. For all three blasts, an average of 64 holes, which were 1 m deep, were drilled and blasted at each step of advance. After each production blast the effectiveness of the round was assessed and the influence of the preconditioning blast was evaluated. The blast-induced fractures were observed and stereo photographs of the face and both sidewalls of the tunnel were taken for fracture-mapping purposes.

After the second test blast, few radial fractures were observed, but the clear effect of the blast was seen by a highly crushed zone (Figure 3.6.2) around the blasthole. After the fifth production blast, there was no indication of fracturing by the preconditioning blast on the tunnel face.

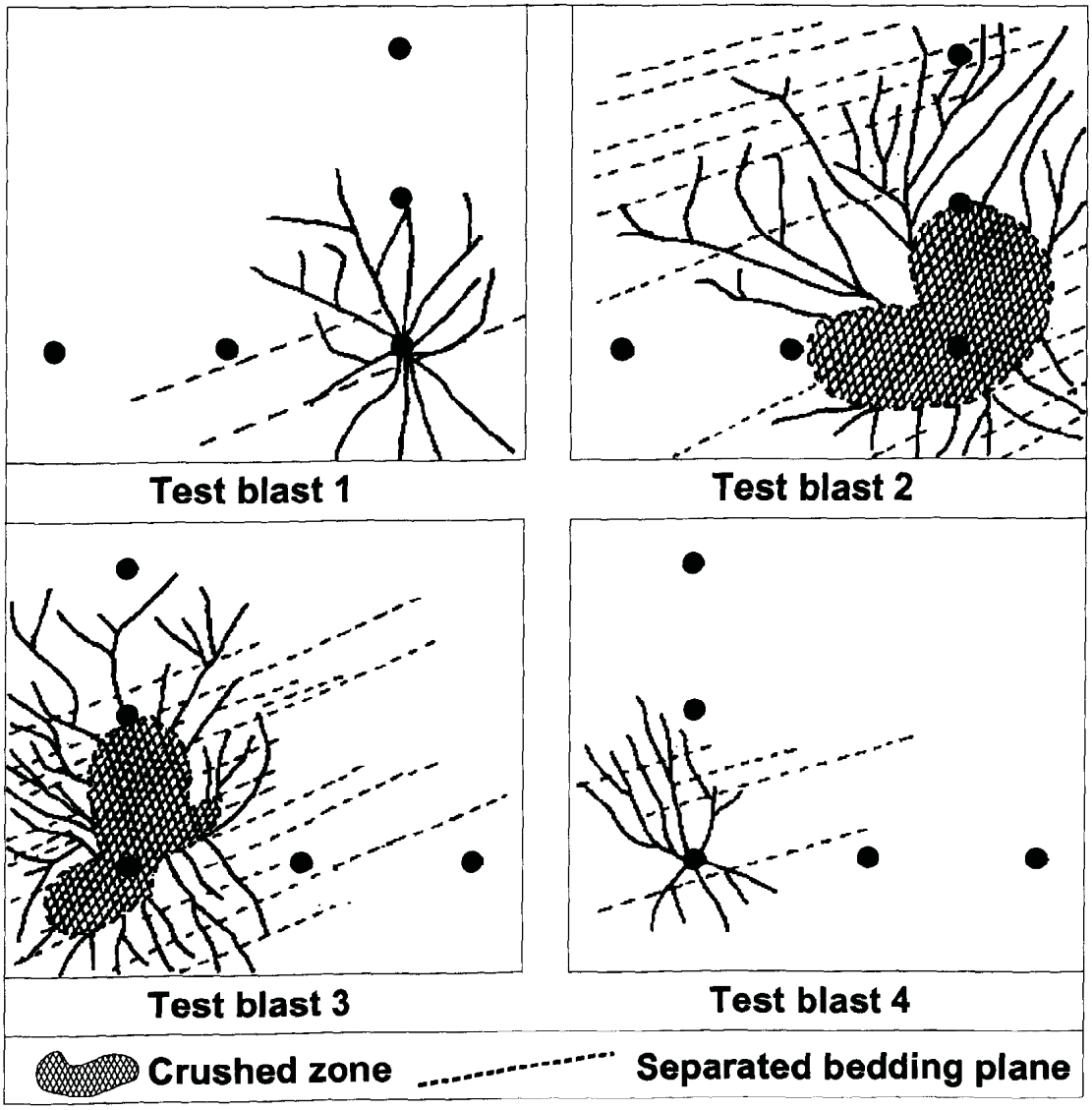

Figure 3.6.2 Schematic view of induced fracturing by test blasts (not to scale)

The observations after the third test blast were similar to those following the second one. After the production blasts, it was observed that the blasthole was completely closed by small pieces of crushed rock through the charge column. A highly fractured zone was observed, as were some radial fractures around the blasthole (Figure 3.6.2). Owing to the effect of the blast, the bedding planes were

opened and visible. Most of the radial fractures were parallel to the major principal stress direction, which was almost perpendicular to the bedding planes.

Unfortunately, the fourth test was a very poor blast. Because of the difficulties that were encountered in using the ANFO loader, the explosive in-hole density was too low and, as a result, the detonation pressure was critically decreased. After each production blast the face was examined, but only a few blast-induced radial fractures were observed around the blasthole. They were all parallel to the major principal stress direction, which was perpendicular to the bedding planes (Figure 3.6.2). The sidewalls of the blasthole were almost intact along its entire length.

3.7 Studies on rock samples

3.7.1 Rock Quality Designation (RQD)

After the second test blast, five BX-size diamond boreholes were drilled at different distances from the blasthole. Rock Quality Designation (RQD) values were determined and compared to the values determined on core samples taken before the preconditioning test blast (Figure 3.7.1). Owing to the effect of the blast, significant decreases in both RQD and the average core length were observed. The average RQD value for 10 holes before the blast was 94 %. However, those values after the blast were calculated as 52 %, 61 % and 82 % at 0.3 m, 0.9 m and 1.5 m respectively away from the blasthole.

Similar studies were carried out before and after the third preconditioning test blast. The average RQD of 92 % before the preconditioning test blast was decreased down to 60 %, 78 % and 88 % at 0.3 m, 0.9 m and 1.5 m away from the blasthole, respectively (Figure 3.7.2).

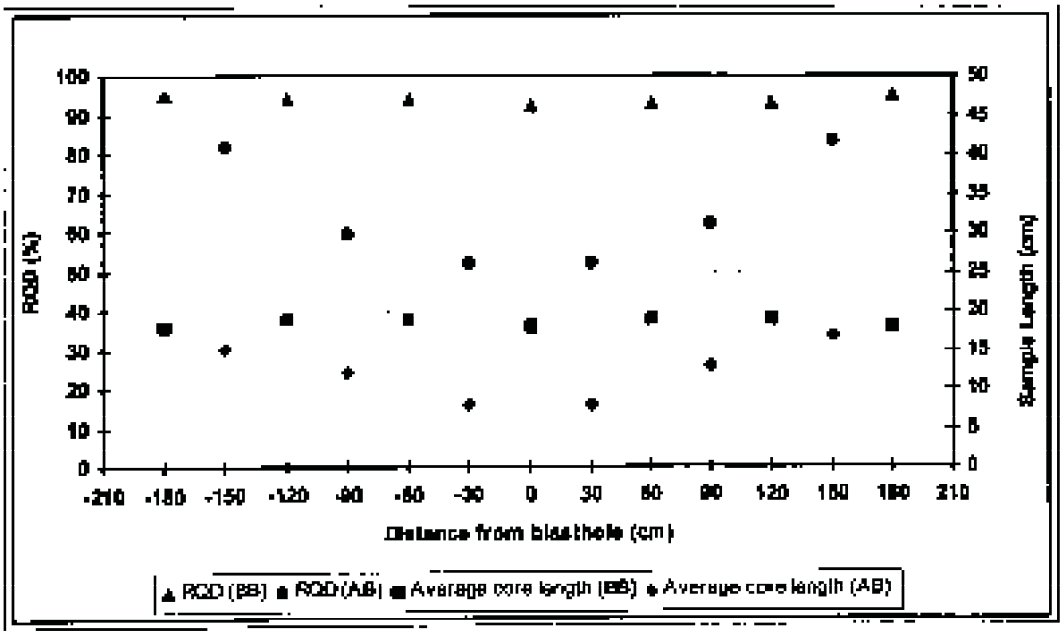

Figure 3.7.1 Rock Quality Designation (RQD) and average core sample lengths, before (BB) and after (AB) the second test blast

Negative values are in the vertical direction and positive values are in the horizontal direction.

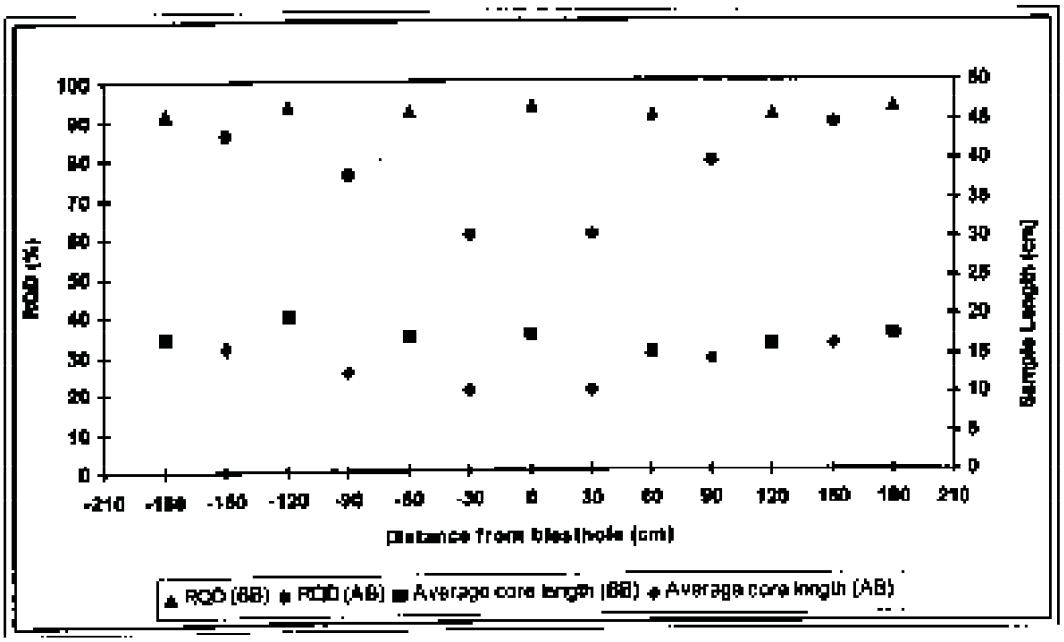

Figure 3.7.2 Rock Quality Designation (RQD) and average core sample lengths, before (BB) and after (AB) the third test blast

Negative values are in the vertical direction and positive values are in the horizontal direction.

3.7.2 Rock testing

Laboratory tests to establish the mechanical properties of rock were carried out on core samples taken before and after the second and third test blasts. Table 3.7.1 summarises the rock testing results. The data shows statistically insignificant changes in intact rock properties as a result of the blasting.

Table 3.7.1 Mechanical properties of intact rock before and after the test blasts

	TEST 2 Before Blast	TEST 2 After Blast	TEST 3 Before Blast	TEST 3 After Blast
Uniaxial Compressive Strength (MPa)	265	256	265	261
Elastic Modulus (GPa)	72	71	71	70
Poisson's Ratio	0.24	0.24	0.18	0.22
Internal Friction Angle (Degrees)	36	37	39	<37

3.8 Stress determination studies

Strain relief measurements (i.e. stress determination) were carried out in the face of the tunnel before the first preconditioning test blast. The maximum principal stresses were calculated as 57 MPa, 47 MPa and 50 MPa at 3.8 m, 4.4 m and 4.6 m ahead of the face respectively, and the minimum principal stresses at the same positions were 27 MPa, 22 MPa and 24 MPa respectively. In order to measure the strain changes brought about by the first test blast, a permanent doorstopper was installed at the end of the 4 m hole which was 1.5 m away from the blasthole, and daily readings were taken on that instrument. Results obtained from those measurements are shown in Figure 3.8.1. It was observed that the first preconditioning test blast had no significant effect on the stress field.

In the second and third preconditioning test blasts, three holes that were located at a diagonal distance of 1 m, 1.5 m and 2 m from the blasthole, were drilled for

the purpose of recording stress changes due to the test blasts. The permanent doorstoppers were installed at the end of each of those three 4 m-deep holes. The strain measurements were done before and after the test blast by taking daily readings.

The doorstopper that was closest (1 m) to the blasthole was damaged by the second test blast and it was not possible to take further measurements from that instrument. The results obtained from the other two doorstoppers are shown in Figure 3.8.2 and Figure 3.8.3. The stress changes in the doorstopper that was 1.5 m away from the blasthole are very large (Figure 3.8.2). However, the measurements from the farthest doorstopper show that the major principal stress is increased by only 15 MPa and that the minor principal stress is decreased by only 3 MPa just after the test blast (Figure 3.8.3).

In order to determine if any major changes in the stress field have occurred during the first half of the programme, a static stress field measurement was carried out in a 4 m-deep hole, before the third test blast. The major and minor principal stresses were measured as 53 MPa and 34 MPa respectively.

After the third preconditioning test blast, the readings on three permanent strain gauges showed a very significant effect on and change in the rock stress regime (Figure 3.8.4, Figure 3.8.5, Figure 3.8.6). The stress changes were calculated by assuming E=71.9 GPa and v=0.23. The stress measurements showed that the major principal stresses were increased by 21 MPa, 15 MPa and 4 MPa, and that the minor principal stresses were decreased by 14 MPa, 6 MPa and 1 MPa at 1 m, 1.5 m and 2 m away from the blasthole respectively, as summarised in Figure 3.8.7.

Final static stress-field measurements were taken just before the fourth test blast. Results showed that the maximum principal stresses were 51 MPa, 60 MPa and 81 MPa at 3.8 m, 4.8 m and 5.8 m ahead of the face respectively, and that the minimum principal stresses at the same positions were 25 MPa, 28 MPa and 53 MPa respectively.

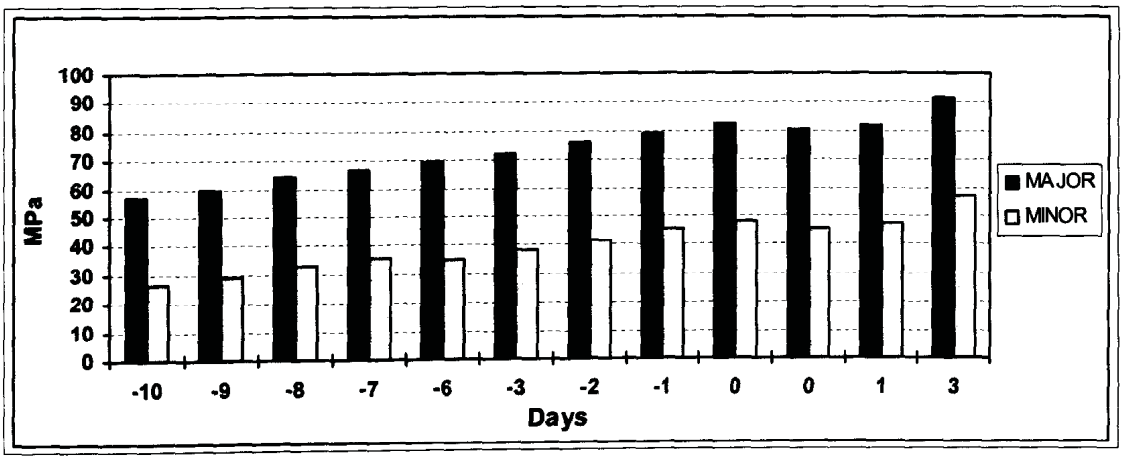

Figure 3.8.1 Principal stresses calculated from strain gauge measurements (1.5 m away from blasthole), Test blast 1

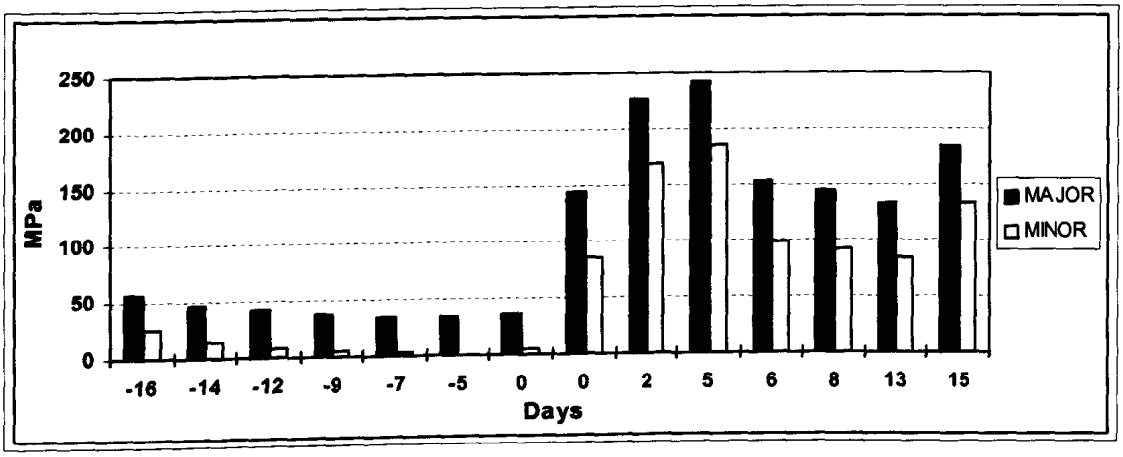

Figure 3.8.2 Principal stresses calculated from strain gauge measurements (1.5 m away from blasthole), Test blast 2

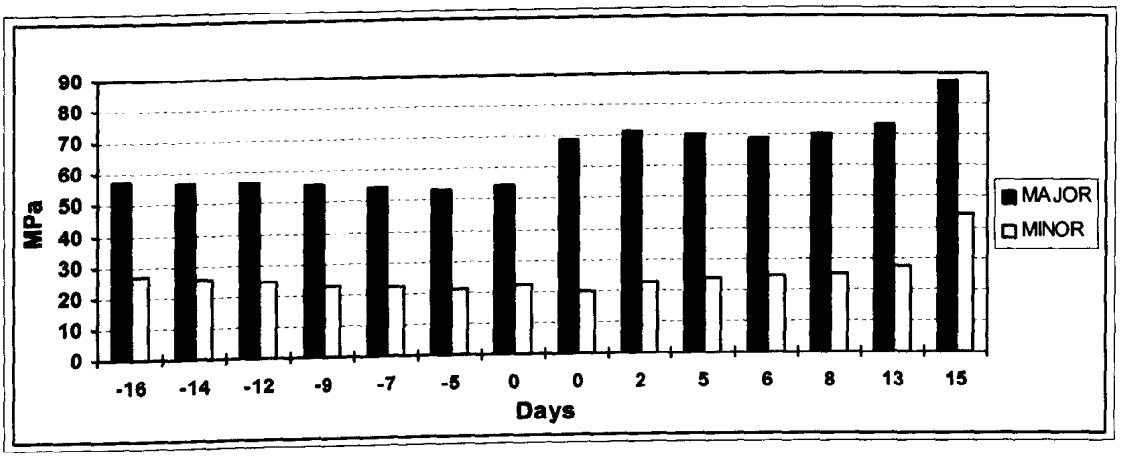

Figure 3.8.3 Principal stresses calculated from strain gauge measurements (2 m away from blasthole), Test blast 2